Journal Marocain de Chimie Hétérocyclique
Moroccan Journal of Heterocyclic Chemistry

ISSN : 2605-5996

J. Mar. Chim. Heterocycl., 2019, Volume 18, Issue 1, Page 43-54

CRYSTAL STRUCTURE AND HIRSHFELD SURFACE ANALYSIS OF 6-BROMO-2-(4-CHLOROPHENYL)-3-((1-OCTYL-1*H*-1,2,3-TRIAZOL-4-YL)METHYL)-3*H*-IMIDAZO[4,5-*b*]PYRIDINE

S. Bourichi[a], Y. Kandri Rodi[a]*, T. Hökelek[b], Y. Ouzidan[a], F. Ouazzani Chahdi[a], M. Akhazzane[c] and E.M. Essassi[d]

[a]*Laboratoire de Chimie Organique Appliquée, Université Sidi Mohamed Ben Abdallah, Faculté des Sciences et Techniques, Route d'immouzzer, BP 2202, Fez, Morocco,*

[b]*Department of Physics, Hacettepe University, 06800 Beytepe, Ankara, Turkey.*

[c]*Cité de l'innovation, Université Sidi Mohammed Ben Abdallah, Fès, Maroc.*

[d]*Laboratoire de Chimie Organique Hétérocyclique, Centre de Recherche des Sciences des Médicaments, Pôle de Compétences Pharmacochimie, URAC 21, Faculté des Sciences, Mohammed V University Rabat, Avenue Ibn Battouta, BP 1014, Rabat, Morocco.*

**Corresponding author. E-mail:* youssef_kandri_rodi@yahoo.fr

Received 10/02/2019, Accepted 05/03/2019.

ABSTRACT

6-bromo-2-(4-chlorophenyl)-3-((1-octyl-1*H*-1,2,3-triazol-4-yl)methyl)-3*H*-imidazo[4,5-*b*] pyridine, is built up from the 4-chlorophenyl and imidazo[4,5-*b*]pyridine ring system linked through a methylene bridge to a 1,2,3-triazole ring, which in turn also carries a substituent. The planar imidazo[4,5-*b*]pyridine ring is inclined by 19.37(12)° and 889.27(13)° to the phenyl and triazole rings, respectively, while phenyl and triazole rings are oriented at a dihedral angle of 71.23(15)°. In the crystal, the molecules are linked *via* intermolecular C—$H_{Trz}\cdots N_{Trz}$ (Trz = triazole) hydrogen bonds, enclosing $R_3^3(21)$ and $R_3^3(22)$ ring motifs, they are further linked through the bifurcated intermolecular C—$H_{Trz}\cdots N_{Trz}$ hydrogen bonds into a network consisting of double-column structure running along the *b*-axis direction. The Hirshfeld surface analysis of the crystal structure indicates that the most important contributions for the crystal packing are from H ⋯ H (57.2%), H ⋯ N/N ⋯ H (17.6%), H ⋯ C/C ⋯ H (9.6%), H ⋯ Cl/Cl ⋯ H (7.9%) and H ⋯ Br/Br ⋯ H (7.0%) interactions. No significant π ⋯ π or C–H ⋯ π interactions are observed.

Keywords : Crystal structure; imidazo[4,5-*b*]pyridine; 1,2,3-triazole; Hirshfeld surface.

1. Structure description

Imidazopyridine derivatives are a very important class of nitrogen-containing fused heterocyclic compounds. Many of the imidazopyridines have a significant inhibitory effect on a lot of target enzymes [1-2], as well as anti-viral, anti-bacterial, anti-microbial and anti-cytokinin activities. Imidazo[4,5-*b*]pyridine derivative are a class of sedative drugs exemplified by *Zolpidem*, *Alpidem*, *Saripidem* and *Necopidem*. On the other hand, they exibit

diverse biological properties such as anticancer [3], tuberculostatic[4] and antimitotic activities [5]. Some of them can be used to treat peptic ulcers, diabetes and mental illness [6-7].The syntheses of imidazo[4,5-b]pyridine derivatives are currently of great interest, and thus a series of the synthetic strategies have been developed to obtain a variety of the substituted structures. The most popular synthetic approach generally involves the cyclocondensation of 2,3-pyridinediamine with carboxylic acid derivatives or with aldehydes [8]. On the other hand, there are much more interest in designing the new synthetic routs in literature; such as, an eco-friendly synthesis by oxidation in aqueous medium has been claimed [9]. Other methods require more than one single step [10-13].

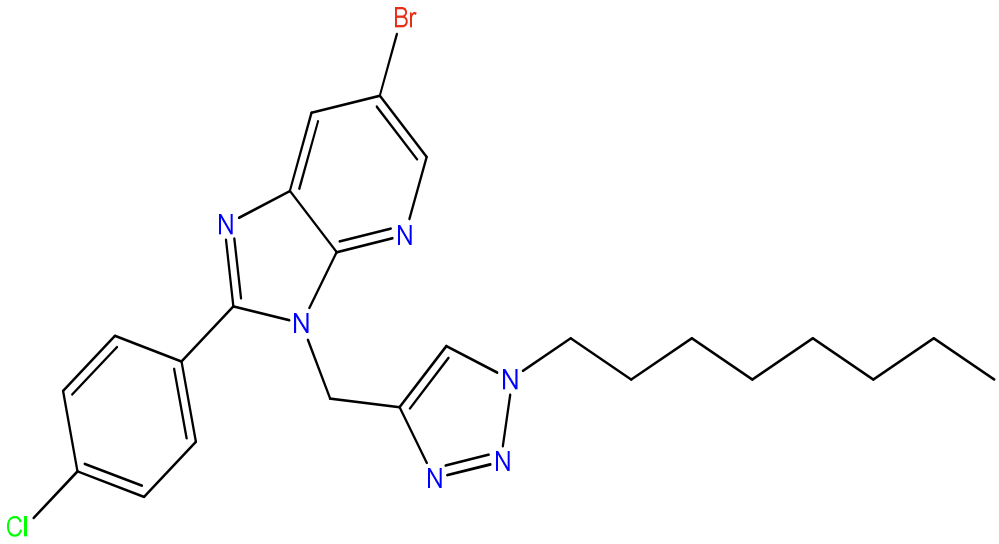

Figure 1

As a continuation of our research devoted to the development of imidazo[4,5-*b*]pyridine derivatives [14,15], we synthesized a new imidazopyridine containing 1,2,3-triazole nucleus by 1,3-cycloaddition reaction. We report herein the molecular and crystal structures along with the Hirshfeld surface analysis of the title compound, 6-bromo-2-(4-chlorophenyl)-3-((1-octyl-1H-1,2,3-triazol-4-yl)methyl) -3H-imidazo[4,5-b]pyridine. (Figure 1).

2. Structural commentary

The title compound, (I), is built up from the 4-chlorophenyl and imidazo[4,5-b]pyridine ring system linked through a methylene bridge to a 1,2,3-triazole ring, which in turn also carries a substituent on N6 atom (Fig. 1). The imidazo[4,5-b]pyridine unit is planar to within -0.026 (5) Å (for atom C7), and the rms deviation of the fitted atoms is 0.0119 Å. It is inclined by 19.37 (12)° and 89.27 (13)° to the phenyl and triazole rings, respectively, while phenyl and triazole rings are oriented at a dihedral angle of 71.23 (15)°. Atoms Br1, Cl1 and C13 and C16 are -0.037 (1) Å, 0.024 (2) Å, and -0.017 (4) Å and 0.031 (5) Å away from the adjacent imidazo[4,5-b]pyridine, phenyl and triazole ring planes, respectively (Fig. 1). Thusthey are co-planar with the corresponding rings.

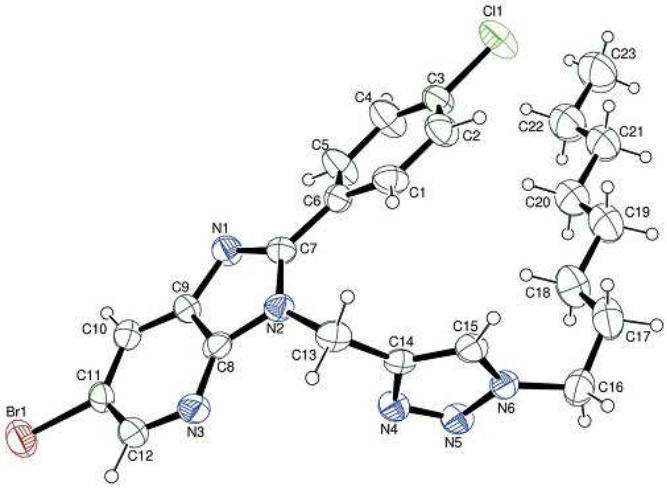

Figure 2. The molecular structure of the title compound with the atom-numbering scheme. Displacement ellipsoids are drawn at the 50% probability level.

3. Supramolecular features

In the crystal, the molecules are linked *via* intermolecular C–H ⋯ N_{Imzpyr} (Imzpyr = imidazo[4,5-b]pyridine) hydrogen bonds (Table 1), enclosing $R_3^3(20)$, $R_3^3(21)$ and $R_3^3(22)$ ring motifs [30] (Figs. 2 and 3), they are further linked through the bifurcated intermolecular C—H_{Trz}⋯N_{Trz} (Trz = triazole) hydrogen bonds (Table 1) into a network consisting of double-column structure (Fig. 2) running along the *b*-axis direction (Fig. 3). The Hirshfeld surface analysis of the crystal structure indicates that the most important contributions for the crystal packing are from H ⋯ H (57.2%), H ⋯ N/N ⋯ H (17.6%), H ⋯ C/C ⋯ H (9.6%), H ⋯ Cl/Cl ⋯ H (7.9%) and H ⋯ Br/Br ⋯ H (7.0%) interactions. Hydrogen bonding and van der Waals interactions are the dominant interactions in the crystal packing. No significant π ⋯ π or C–H ⋯ π interactions are observed.

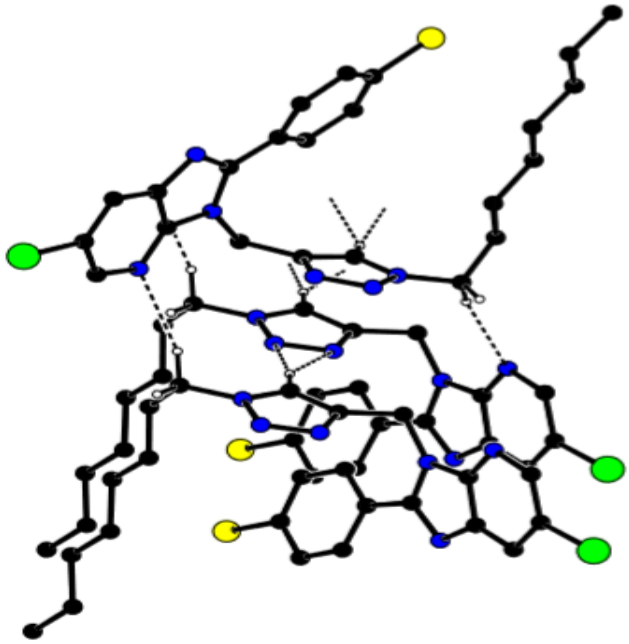

Figure 3. Part of the crystal structure. C–H ⋯ N_{Imzpyr} and bifurcated C–H_{Trz} ⋯ N_{Trz} (Imzpyr = imidazo[4,5-*b*]pyridine and Trz = triazole) hydrogen bonds, enclosing $R_3^3(20)$, $R_3^3(21)$ and $R_3^3(22)$ ring motifs, are shown as dashed lines. Non-bondinghydrogenatoms have been omitted for clarity.

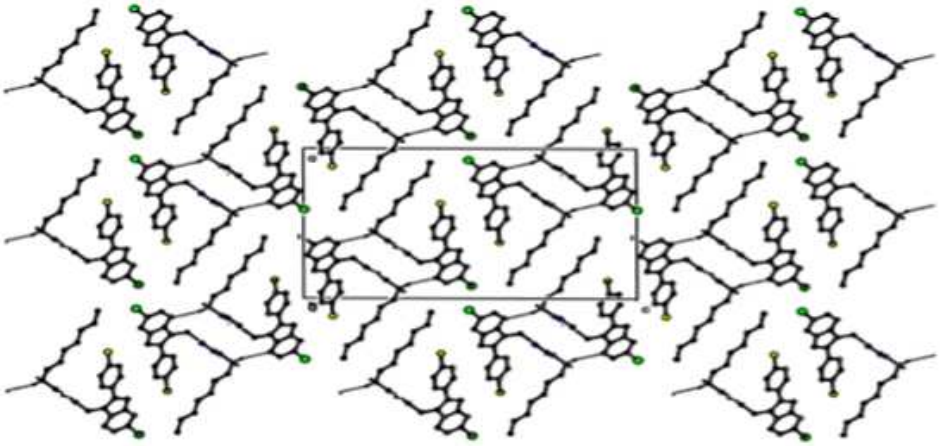

Figure 4. Packing viewed along the *b*-axis direction. C–H ⋯ N_{Imzpyr} hydrogen bonds are shown by dashed lines.

Table 1 Experimentaldetails

	Compound (I)
Crystal data	
Chemical formula	$C_{23}H_{26}BrClN_6$
M_r	501.86
Crystal system, space group	Monoclinic, $P2_1/n$
Temperature (K)	296
a, *b*, *c* (Å)	16.252 (3), 5.3787 (9), 27.109 (4)
β (°)	90.551 (12)
V (Å^3)	2369.6 (7)
Z	4
Radiation type	Mo *Kα*
μ (mm^{-1})	1.87
Crystal size (mm)	0.26 × 0.06 × 0.04
Data collection	
Diffractometer	Bruker*APEX*-II CCD
Absorption correction	Multi-scan *SADABS2016*/2 (Bruker,2016/2) was used for absorption correction. wR2(int) was 0.0955 before and 0.0504 after correction. The Ratio of minimum to maximum transmission is 0.8888. The λ/2 correction factor

	is Not present.
T_{min}, T_{max}	0.662, 0.745
No. of measured, independent and observed [$I > 2\sigma(I)$] reflections	26673, 4359, 2265
R_{int}	0.074
$(\sin \theta/\lambda)_{max}$ (Å^{-1})	0.604
Refinement	
$R[F^2 > 2\sigma(F^2)]$, $wR(F^2)$, S	0.053, 0.124, 1.01
No. of reflections	4359
No. of parameters	281
H-atomtreatment	H-atomparametersconstrained
$\Delta\rho_{max}$, $\Delta\rho_{min}$ (e Å^{-3})	0.26, −0.27

Computer programs: *APEX2*[17], *SAINT* v8.37A [18], *SHELXT*[19], *SHELXL-2018/1*[20], *ORTEP-3* for Windows [21], *WinGX* publication routines [21]and *PLATON*[22].

4. Refinement

The experimental details including the crystal data, data collection and refinement are summarized in Table 2. The C-bound H-atoms were positioned geometrically with C—H = 0.93, 0.97 and 0.96 Å for aromatic, methine and methyl hydrogens and refined as riding with $U_{iso}(H) = k \times U_{eq}(C)$, where k = 1.2 for aromatic and methine H atoms and k = 1.5 for methyl H atoms.

For more crystallographic data see [23]. The supplementary crystallographic data for these compounds can be obtained free of charge from the Cambridge Crystallographic Data Centre via http://www.ccdc.cam.ac.uk/data_request/cif. CCDC N° 1889816.

Table 2 Selected interatomic distances (Å)

Br1···Br1^{i}	3.9848 (11)	C1···C15	3.470 (7)
Br1···C8^{ii}	3.602 (5)	C1···H13B	2.8421
Br1···C9^{ii}	3.721 (5)	C2···C5^{iv}	3.555 (8)
Br1···C12^{i}	3.744 (5)	C5···C5^{v}	3.585 (7)
Br1···H23A^{iii}	3.1643	C5···H5^{v}	2.8073
Cl1···H20A^{iv}	3.0344	C6···C14	3.488 (6)
N1···H5	2.4424	C13···H1	2.6541

N1···H4^{v}	2.6950	C14···H1	2.9415
N2···N4	2.954 (5)	C15···H17A	2.9546
N2···H1	2.9070	H1···H13B	2.0808
N3···C16^{vi}	3.444 (6)	H4···H5^{v}	2.5846
N3···H13A	2.5390	H5···H5^{v}	2.1546
N3···H16B^{vi}	2.5313	H16A···H18B	2.5168
N4···C1^{ii}	3.442 (6)	H17A···H19A	2.5867
N4···C15^{ii}	3.452 (6)	H17B···H19B	2.4611
N4···H1^{ii}	2.7057	H18A···H20A	2.5558
N4···H15^{ii}	2.5983	H18B···H20B	2.4450
N5···C15^{ii}	3.293 (6)	H19A···H21A	2.5951
N5···H15^{ii}	2.3782	H19B···H21B	2.5465
N6···H18A	2.7164	H20A···H22A	2.4691
C1···C9^{iv}	3.570 (7)	H20B···H22B	2.4704
C1···C13	3.225 (7)	H21A···H23C	2.5052
C1···C14	3.365 (6)	H21B···H23B	2.5978

Symmetrycodes: (i) −*x*+2, −*y*+2, −*z*+1; (ii) *x*, *y*+1, *z*; (iii) −*x*+1, −*y*+2, −*z*+1; (iv) *x*, *y*−1, *z*; (v) −*x*+1, −*y*+1, −*z*+1; (vi) −*x*+3/2, *y*+1/2, −*z*+3/2.

5. Hirshfeld surface analysis

In order to visualize the intermolecular interactions in the crystal of the title compound, a Hirshfeld surface (HS) analysis [24-25] was carried out by using *Crystal Explorer 17.5*[26]. In the HS plotted over d_{norm} (Fig. 5), the white surface indicates contacts with distances equal to the sum of van der Waals radii, and the red and blue colours indicate distances shorter (in close contact) or longer (distinct contact) than the van der Waals radii, respectively [27].

The bright-red spots appearing near N3, N4, N5 and hydrogen atom H15 indicate their roles as the respective donors and/or acceptors in the dominant C–H ··· N hydrogen bonds; they also appear as blue and red regions corresponding to positive and negative potentials on the HS mapped over electrostatic potential [28-29] as shown in Fig.6. The blue regions indicate the positive electrostatic potential (hydrogen-bond donors), while the red regions indicate the negative electrostatic potential (hydrogen-bond acceptors). The shape-index of the HS is a tool to visualize the π ··· π stacking by the presence of adjacent red and blue triangles; if there are no adjacent red and/or blue triangles, then there are no π ··· π interactions. Fig. 7 clearly suggest that there is no π ··· π interactions in (I). The overall two-dimensional fingerprint plot, Fig. 7*a*, and those delineated into H ··· H, H ··· N/N ··· H, H ··· C/C ··· H, H ··· Cl/Cl ··· H,

H ⋯ Br/Br ⋯ H, C ⋯ Br/Br ⋯ C, N ⋯ C/C ⋯ N, C ⋯ C, Br ⋯ Br, N ⋯ Br/Br ⋯ N and N ⋯ Cl/Cl ⋯ N contacts[30] are illustrated in Figs. 8 *b-l*, respectively, together with their relative contributions to the Hirshfeld surface. The most important interaction is H ⋯ H contributing 47.2% to the overall crystal packing, which is reflected in Fig. 8*b* as widely scattered points of high density due to the large hydrogen content of the molecule. The spike with the tip at $d_e = d_i = 0.98$ Å in Fig. 8*b* is due to the short interatomic H ⋯ H contacts (Table 3). The pair of characteristic wings resulting in the fingerprint plot delineated into H ⋯ N/N ⋯ H contacts Fig. 7*c*, the 17.6% contribution to the HS arises from the C–H ⋯ N hydrogen bonds (Table 1) as well as from the H ⋯ N/N ⋯ H contacts (Table 3) and is wieved as pair of spikes with the tips at $d_e + d_i = 2.22$ Å.In the absence of C–H ⋯ π interactions, the pair of widely scattered points of wings resulting in the fingerprint plot delineated into H ⋯ C/C ⋯ H contacts with 9.6% contribution to the HS have a nearly symmetrical distribution of points, Fig. 7*d*, with the tips at $d_e + d_i$ 3.17 Å arising from the the H ⋯ C/C ⋯ H contacts (Table 3). The H ⋯ Cl/Cl ⋯ H (Fig. 7*e*) contacts (Table 3) in the structure with 7.9% contribution to the HS also have symmetrical distribution of points, and the pairs of spikes with the tips at $d_e + d_i = 2.94$ Å, result from the interatomic H ⋯ Cl/Cl ⋯ H contacts (Table 3). The H ⋯ Br/Br ⋯ H (Fig. 8*f*) contacts (Table 3) in the structure with 7.0% contribution to the HS have unsymmetrical distribution of points, and the pairs of spikes with the tips at $d_e + d_i = 3.02$ Å, result from the interatomic H ⋯ Br/Br ⋯ H contacts (Table 3). The C ⋯ Br/Br ⋯ C (Fig. 8*g*) contacts (Table 3) in the structure with 3.5% contribution to the HS have symmetrical distribution of points, and the pairs of spikes with the tips at $d_e + d_i = 3.58$ Å, result from the interatomic C ⋯ Br/Br ⋯ C contacts (Table 3). Finally, the N ⋯ C/C ⋯ N (Fig. 8*h*) contacts (Table 3) in the structure with 2.5% contribution to the HS also have symmetrical distribution of points, and the pairs of spikes with the tips at $d_e + d_i = 3.38$ Å, result from the interatomic N ⋯ C/C ⋯ N contacts (Table 3).

The Hirshfeld surface representations with the function d_{norm} plotted onto the surface are shown for the H ⋯ H, H ⋯ N/N ⋯ H, H ⋯ C/C ⋯ H, H ⋯ Cl/Cl ⋯ H, H ⋯ Br/Br ⋯ H and C ⋯ Br/Br ⋯ C interactions in Fig. 9*a-f*, respectively.

The Hirshfeld surface analysis confirms the importance of H-atom contacts in establishing the packing. The large number of H ⋯ H, H ⋯ N/N ⋯ H and H ⋯ C/C ⋯ H interactions suggest that van der Waals interactions and hydrogen bonding play the major roles in the crystal packing [31].

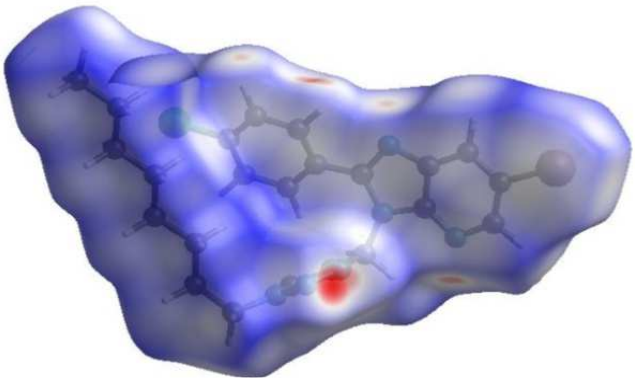

Figure 5. View of the three-dimensional Hirshfeld surface of the title compound plotted over d_{norm} in the range -0.3131 to 1.3886 a.u.

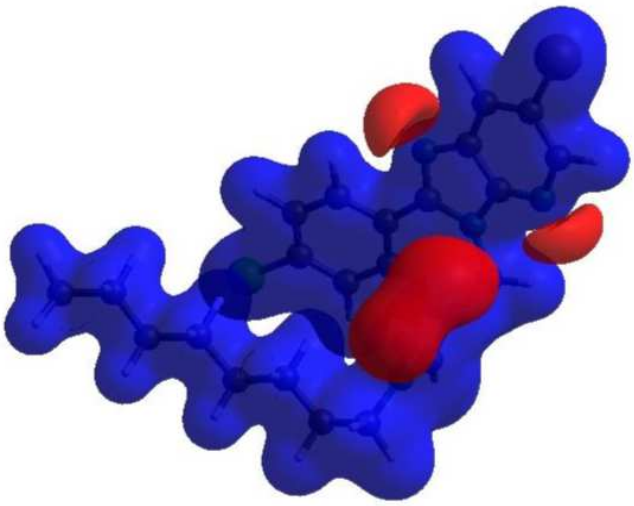

Figure 6. View of the three-dimensional Hirshfeld surface of the title compound plotted over electrostatic potential energy in the range -0.0500 to 0.0500 a.u. using the STO-3 G basis set at the Hartree–Fock level of theory hydrogen-bond donors and acceptors are shown as blue and red regions around the atoms corresponding to positive and negative potentials, respectively.

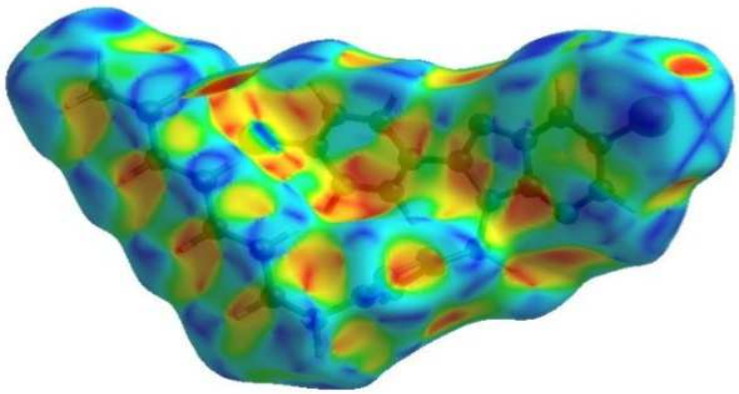

Figure 7. Hirshfeld surface of the title compound plotted over shape-index.

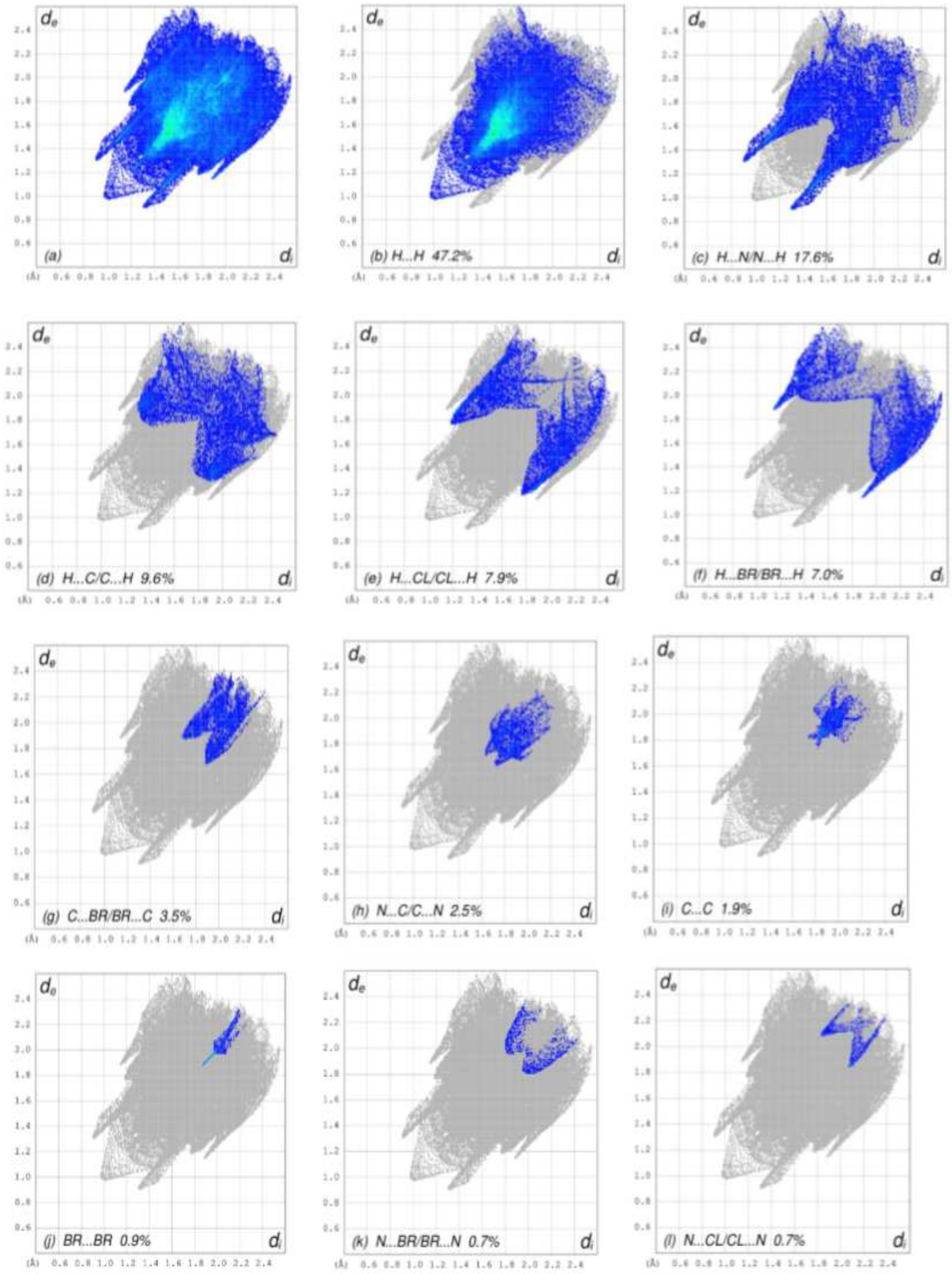

Figure 8. The full two-dimensional fingerprint plots for the title compound, showing (*a*) all interactions, and delineated into (*b*) H ⋯ H, (*c*) H ⋯ N/N ⋯ H, (*d*) H ⋯ C/C ⋯ H, (*e*) H ⋯ Cl/Cl ⋯ H, (*f*) H ⋯ Br/Br ⋯ H, (*g*) C ⋯ Br/Br ⋯ C, (*h*) N ⋯ C/C ⋯ N, (i) C ⋯ C, (*j*) Br ⋯ Br, (*k*) N ⋯ Br/Br ⋯ N, and (*l*) N ⋯ Cl/Cl ⋯ N, interactions. The d_i and d_e values are the closest internal and external distances (in Å) from given points on the Hirshfeld surface contacts.

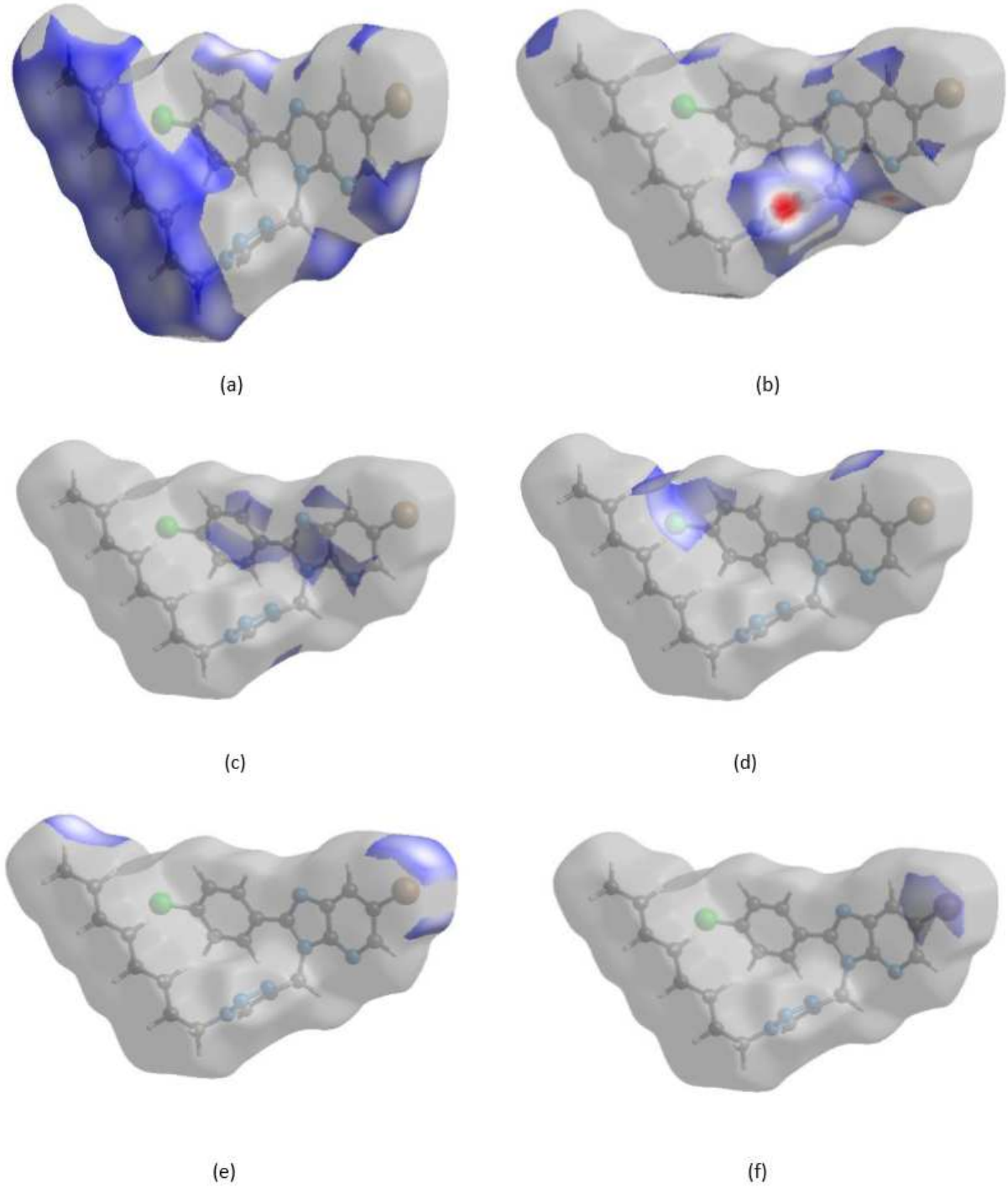

Figure 9. The Hirshfeld surface representations with the function d_{norm} plotted onto the surface for (*a*) H ⋯ H, (*b*) H ⋯ N/N ⋯ H, (*c*) H ⋯ C/C ⋯ H, (*d*) H ⋯ Cl/Cl ⋯ H, (*e*) H ⋯ Br/Br ⋯ H and (*f*) C ⋯ Br/Br ⋯ C interactions.

Table 3 Hydrogen-bond geometry (Å, °)

D—H···*A*	*D*—H	H···*A*	*D*···*A*	*D*—H···*A*
C15—H15···N4^{iv}	0.9300	2.6000	3.452 (6)	153.00
C15—H15···N5^{iv}	0.9300	2.3800	3.293 (6)	168.00
C16—H16B···N3^{vii}	0.9700	2.5300	3.444 (6)	157.00

Symmetrycodes: (iv) *x*, *y*−1, *z*; (vii) −*x*+3/2, *y*−1/2, −*z*+3/2.

7. Synthesis and crystallization

To a solution of 6-bromo-2-(4-chlorophenyl)-3-(prop-2-yn-1-yl)-3H-imidazo[4,5-b] pyridine (0.2 g, 0.58 mmol) in ethanol (20 ml) was added 1-azidooctane (0.18 mg, 1.16 mmol). The mixture was stirred under reflux for 48 h. After completion of reaction (monitored by TLC), the solution was concentrated and the residue was purified by column chromatography on silica gel by using a mixture (hexane/ethyl acetate 3/1). Crystals were obtained when the solvent was allowed to evaporate.

8. Acknowledgements

T. H. is grateful to Hacettepe University Scientific Research Project Unit (Grant No. 013 D04 602 004).

References

[1] A. M. Palmer, B. Grobbel, C. Jecke, C. Brehm, P. J. Zimmermann, W. Buhr, M. P. Feth, W. A. Simon, & W. Kromer, *J. Med. Chem.***50**, 6240–6264. (2007)

[2] A. R. Katritzky, Y. J. Xu & H. Tu, *J. Org. Chem.***68**, 4935–4937 (2003).

[3] P. M. Lukasik, S. Elabar, F. Lam, H. S. Xiangrui Liu, A. Y. Abbas & S. Wang, *Eur. J. Med. Chem.***57**, 311–322 (2012).

[4] L. Bukowski & M. Janowiec, *Pharmazie*, **44**, 267–269. (1989).

[5] G. Aridoss, S. Balasubramanian, P. Parthiban, S. Kabilan (2006). *Eur. J. Med. Chem.***41**, 268–275.

[6] A. Scribner, R. Dennis, J. Hong, S. Lee, D. McIntyre, D. Perrey, D. Feng, M. Fisher, M. Wyvratt, P. Leavitt, P. Liberator, A. Gurnett, C. Brown, J. Mathew, D. Thompson, D. Schmatz, T. Biftu, *Eur. J. Med. Chem.***42**, 1334–1357 (2007).

[7] G. B. Liang, X. Qian, D. Feng, M. Fisher, C. M. Brown, A. Gurnett, P. S. Leavitt, P. A. Liberator, A. S. Misura, T. Tamas, D. M. Schmatz, M. Wyvratt, & T. Biftu, *Bioorg. Med. Chem. Lett.***17**, 3558–3561 (2007).

[8] P. K. Dubey, R. V. Kumar, S. M. Kulkarni, H. G. Sunder, G. Smith & C. H. L. Kennard, *Indian J. Chem.* B**43**, 952–956 (2004).

[9] R. P. Kale, M. U. Shaikh, G. R. Jadhav, & C. H. Gill, *Tetrahedron Lett.***50**, 1780–1782. (2009).

[10] C. D. Benham, T. P. Blackburn, A. Johns, N. R. Kotecha, R. T. Martin, D. R. Thomas, M. Thompson, & R. W. Ward, *Bioorg. Med. Chem. Lett.***5**, 2455–2460. (1995).

[11] D. J. Cundy, G. Holan, M. Otaegui, & G. W. Simpson, *Bioorg. Med. Chem. Lett.***7**, 669–674. (1997).

[12] T. F. Walsh, K. J .Fitch, M. MacCoss, R. S. L. Chang, S. D. Kivlighn, V. J. Lotti, P. K. S. Siegl, A. Patchett, & W. J. Greenlee, *Bioorg. Med. Chem. Lett.***4**, 219–222 (1994).

[13] M. E. A. Zaki & M. F. Proença, *Tetrahedron*, **63**, 3745–3753. (2007).

[14] S. Bourichi, Y. Kandri Rodi, Y. Ouzidan, T. J. Mague, E. M. Essassi & H. Zouihri, *IUCrData*, **1**, x160763 (2016).
[15] Y. Ouzidan, S. Obbade, F. Capet, E. M. Essassi & S. W. Ng, *Acta Cryst.*E**66**, o946. (2010).
[16] J. Bernstein, R. E. Davis, L. Shimoni & N. L. Chang, *Angew. Chem. Int. Ed. Engl.* **34**, 1555–1573 (1995).
[17] Bruker (2015). *APEX2*, *SAINT*&*SHELXTL*, Madison, WI.
[18] Bruker (2016). *SADABS*, Madison, WI.
[19] G. M. Sheldrick, *SHELXT*. *Acta Cryst.* A**71**, 3-8. (2015).
[20] G. M. Sheldrick, *SHELXL-2014/7*. *Acta Cryst.* C**71**, 3-8. (2015).
[21] L. J. Farrugia, *J. Appl. Cryst.***45**, 849–854. (2012).
[22] A. L. Spek, *Acta Cryst.*C**71**, 9–18. (2015).
[23] S. Bourichi, Y. Kandri Rodi, T. Hökelek, S. Chakroune, Y. Ouzidan and F. Capet, *IUCrData* 4, x190053 (2019).
[24] H. L. Hirshfeld, *Theor. Chim. Acta*, **44**, 129–138. (1977).
[25] M. A. Spackman, & D. Jayatilaka, *CrystEngComm*, **11**, 19–32. (2009).
[26] M. J. Turner, J. J. McKinnon, S. K. Wolff, D. J. Grimwood, P. R. Spackman, D. Jayatilaka, & M. A. Spackman, *CrystalExplorer17*. The University of Western Australia. (2017).
[27] P. Venkatesan, S. Thamotharan, A. Ilangovan, H. Liang, & T. Sundius, *Spectrochim. Acta Part A*, **153**, 625–636. (2016).
[28] M. A. Spackman, J. J. McKinnon & D. Jayatilaka, *CrystEngComm*, **10**, 377–388. (2008).
[29] D. Jayatilaka, D. J. Grimwood, A. Lee, A. Lemay, A. J. Russel, C. Taylor, S. K. Wolff, , P. Cassam-Chenai & A. Whitton, *TONTO - A System for Computational Chemistry.* (2005).
[30] J. J. McKinnon, D. Jayatilaka & M. A. Spackman, *Chem. Commun.* 3814–3816. (2007).
[31] V. R. Hartwar, M. Sist, M. R. V. Jorgensen, A. H. Mamakhel, X. Wang, C. M. Hoffmann, K. Sugimoto, J. Overgaard & B. B. Iversen, *IUCrJ*, **2**, 563–574 (2015).